Environmental Engineering and Management Journal *June 2021, Vol. 20, No. 6, 871-881*
http://www.eemj.icpm.tuiasi.ro/; http://www.eemj.eu

"Gheorghe Asachi" Technical University of Iasi, Romania

REMOVAL OF VANADIUM IONS FROM AQUEOUS SOLUTIONS USING DIFFERENT TYPE OF HYDROXYAPATITES: ADSORPTION ISOTHERM, KINETICS AND THERMODYNAMIC STUDIES

Inga Zinicovscaia[1,2]*, Nikita Yushin[1], Daler Abdusamadzoda[1], Dmitrii Grozdov[1], Ionel Humelnicu[3], Maria Ignat[3], Doina Humelnicu[3]

[1]Department of Nuclear Physics, Joint Institute for Nuclear Research, Joliot-Curie Str. 6, Dubna, 141980, Russia
[2]Department of Nuclear Physics, Horia Hulubei National Institute for R&D in Physics and Nuclear Engineering, Bucharest - Magurele, Romania
[3]"Alexandru Ioan Cuza" University of Iasi, Faculty of Chemistry, Iasi, Romania

Abstract

Removal of vanadium (V) by hydroxyapatite and its two modifications under different pH, contact time, vanadium concentration, and the temperature has been evaluated. The maximum removal of vanadium ions was achieved at pH 2.0. Four kinetic models (pseudo-first-order, pseudo-second-order, Elovich, and intraparticle diffusion model) and three isotherm models (Langmuir, Freundlich, and Temkin) were used to describe the adsorption kinetics and adsorption equilibrium data. The maximum adsorption capacity was obtained for hydroxyapatite treated with Pluronic P123 (24.1 mg/g), followed by hydroxyapatite treated with Pluronic F127 (14.20 mg/g) surfactant and untreated hydroxyapatite (18.10 mg/g). The standard free energy ($\Delta G°$), enthalpy ($\Delta H°$), and entropy ($\Delta S°$) were calculated to understand the nature of the adsorption process.

Keywords: adsorption, atomic absorption spectrometry, hydroxyapatite, vanadium

Received: March, 2020; Revised final: September, 2020; Accepted: October, 2020; Published in final edited form: June, 2021

1. Introduction

The necessity of vanadium removal from wastewater is determined by its wide application in industry and high toxicity for living organisms. Vanadium causes a variety of toxic effects such as hematological and biochemical changes, neurobehavioral injury, abnormalities in development and reproduction, morphological and functional lesions in organs (Zwolak, 2020). Vanadium exists in the environment as tetravalent [V(IV)] and pentavalent [V(V)] forms of which the pentavalent form is more toxic than the tetravalent one (Sharififard and Soleimani 2015). Nowadays, vanadium and its compounds are discharged in natural water by industries such as glass, textile, ceramic, photography, metallurgy, rubber, and plants producing industrial inorganic chemicals (mainly phosphoric acid) and pigments (He et al., 2018; Sharififard and Soleimani, 2015). Vanadium is also discharged into the environment from oil refineries and power plants in the form of vanadium-rich oil fuel and coal (Sharififard and Soleimani 2015). Thus, its removal before effluent discharge in natural water is extremely important. Literature describing the removal of vanadium from contaminated aquatic systems is rather limited (Peng et al., 2017; Sharififard and Soleimani 2015; Vega et al., 1999; 2003).

The traditional methods for vanadium recovery include chemical precipitation with an ammonium salt, ion exchange, and solvent extraction. The application of these techniques is limited by the

* Author to whom all correspondence should be addressed: e-mail: zinikovskaia@mail.ru; Phone: +74962165609; Fax: +74962165089

release of NH_4^+-N in the water and low efficiency at low vanadium concentration of the solution (Peng et al., 2017). Adsorption can be considered as an economic and highly effective method of metal removal, especially when low-cost sorbents with high sorption capacity are used (Bazargan-Lari et al., 2014).Hydroxyapatite (HAP), $Ca_{10}(PO_4)_6(OH)_2$, is considered to be the most stable form of calcium phosphate and an environmentally benign functional material (Bazargan-Lari et al., 2014; Paz et al., 2012). HAP has attracted a great deal of attention in water treatment due to its high capacity for the removal of heavy metal ions, low water solubility, high stability under reducing and oxidizing conditions, availability, and low cost (Bazargan-Lari et al., 2014). The synthesis of morphologically different HAP has become an interesting area in the field of HAP chemistry since it allows to improve their mechanical strength and increase adsorption capacity (Paz et al., 2012; Wang et al., 2019; Wang et al., 2010).

Hydroxyapatite/chitosan (N-HAP/chitosan) composite was used for treating the solutions containing Cu(II). The maximum adsorption capacity of sorbent was found to be 1.776 mmol/g (Bazargan-Lari et al., 2014). The combination of HAP with the bacterial strains led to higher adsorption capacity for Zn(II), Cd(II) (Piccirillo et al., 2013). It was reported that composite sorbents made via *in situ* incorporation of 2.5 wt% nitrilotris (methylene) triphosphonic acid molecules in the HAP, demonstrated better zinc and lead sorption than HAP alone, by 30.7% for zinc and 47.5% for lead (Saoiabi et al., 2016). A significant increase in lead sorption capacity of needle-like HAP (83 mg/g) in comparison with HAP coated granular activated carbon (14 mg/g) was reported by Fernando et al. (2015). P123 and F127 are triblock copolymers formed by packing hydrophilic poly(ethylene oxide) with hydrophobic poly(propylene oxide), which can form micelles of different forms and sizes in various solvents. In the present study, they were used as structure-directing agents. They act as porogens and induce pores/voids in the hydroxyapatite structure. When the HA precipitated around the formed micelles in the reaction mixture, the structure-directing agents were removed by high thermal treatment, living behind voids, thus enhancing the material porosity.

The present study aimed to test the sorption properties of hydroxyapatite and its two modifications, HAP P123 and HAP F127, in the removal of vanadium(V) ions from aqueous solution at different pH, contact time, temperature, and initial vanadium concentration. Several kinetic and equilibrium models were applied to describe the adsorption process and thermodynamic studies were performed to reveal the nature of the process.

2. Materials and methods

-

2.1. Reagents

Calcium nitrate, sodium orthovanadate and phosphoric acid as well as surfactants (Pluronic P123 and Pluronic F127) were purchased from Sigma Aldrich. Ethylic alcohol and liquid ammonia were purchased from a Chemical Company.

2.2. Sorbents synthesis

Hydroxyapatite (HAP) was obtained by co-precipitation of calcium nitrate and phosphoric acid according to the procedure described by Arsad et al. (2011) with some modifications. The aqueous solution of 0.5 M calcium nitrate was added to 50 mL ethanol and was vigorously stirred at room temperature. The pH of the solution was adjusted to 10 by the addition of 25% (v/v) ammonia in the solution. The 0.3 M phosphoric acid was added slowly in a dropwise manner to allow reacting with calcium nitrate. After 1 h reaction at 60°C, the reaction mixture was kept to age overnight at room temperature to complete the reaction. Then, the suspension was centrifuged at 4,000 rpm for 15 min, separated, and dried at room temperature. The white powder of the sample was calcined for 6 hours at 550ºC and labeled as HAP. The synthesized hydroxyapatite ($Ca_{10}(PO_4)_6(OH)_2$) maintains its stability at the temperature applied for calcination. According to Ramanan and Venkatesh (2004), the adsorbed water is removed from the hydroxyapatite surface at temperature < 200ºC, from the pores up to 500ºC, and the structural water is removed at temperature > 900ºC. Also, it is well known that the TCP-tricalcium phosphates ($Ca_3(PO_4)_2$) phase appear at temperatures > 700°C (Liu et al., 2001).

The HAP P123 and HAP F127 sorbents were obtained following the same procedure except that the corresponding surfactants were added to the reaction mixture (before calcination). Thus, the pluronic P123 has been used to synthesize the HAP P123 sample, and pluronic F127 to synthesize HAP F127. At the calcination temperature of 550 ºC, the surfactants P12 $(HO(CH_2CH_2O)_{20}(CH_2CH(CH_3)O)_{69}(CH_2CH_2O)_{20}H)$ and F127 $(HO(CH_2CH_2O)_{100}(CH_2CH(CH_3)O)_{65}(CH_2CH_2O)_{100}H)$ were decomposed to CO_2 and H_2O, leaving behind pores. Since the surfactants are block copolymers, they are not combusted at such high temperature.

The synthesis of sorbent material was run in duplicate. The reproducibility of the prepared materials was proven by N_2-sorption, which allows the evaluation of the specific surface area of sorbents. For both repetitions, the textural parameter had the same value. To calculate the Ca/P ratio concentrations of Ca and P in synthesized sorbents were measured using atomic absorption spectrometry.

2.3. Sorption experiments

The effect of pH (2.0-6.0), time (5-150 min), vanadium concentration (10-100 mg/L) and temperature (20-50ºC) on vanadium sorption from synthetic wastewaters was carried out. The adsorption experiments were performed placing 0.02 g of sorbent

in a 50 mL flask with 10 mL of a solution containing vanadium at constant agitation. After experiments, sorbent was separated from the solution by filtration and vanadium concentration in solution was determined. Experiments were performed in triplicate and the average of measurements was used in the calculation.

The vanadium uptake q was calculated using the Eq. (1):

$$q = \frac{(C_i - C_f)V}{m} \quad (1)$$

Removal efficiency, R (%) from the Eq. (2):

$$R = \frac{C_i - C_f}{C_i} \cdot 100\% \quad (2)$$

where q is the amount of metal ions adsorbed on the sorbent, mg/g; V is the volume of solution, ml; C_i is the initial concentration of metal in mg/L; C_f is the final metal concentration in the solution, mg/L; m is the mass of sorbent, g.

2.4. Methods

The N_2 adsorption/desorption isotherms for BET specific surface area measurements were recorded on a NOVA 2200e (Quantachrome Instruments) automated gas adsorption analyzer. Before analysis, the samples were outgassed at 120°C for at least 6 h under vacuum. Adsorbents surface analysis was performed using the S3400N Scanning Electron Microscope (Hitachi, USA).

Vanadium concentration in solution was determined by applying atomic absorption spectrometry (Thermo Scientific iCE 3400 series, USA) with electrothermal atomization. The calibration solutions were prepared from a 1 g/L stock solution (AAS standard solution; Merck, Germany). Infrared spectra were recorded in the range of 4,000–400 cm^{-1} using a Bruker Alpha Platinum-ATR spectrometer (Bruker Optics, Ettingen, Germany).

3. Results and discussion

3.1. Sorbents characterization

The ratio of Ca/P in the obtained hydroxyapatite materials according to measured concentrations in the present study was 1.67. The nitrogen adsorption/desorption isotherms for HAP and its two modifications are presented in Fig. 1. Obtained results show the increase in the slope of the isotherm at $P/P_0 > 0.4$.

According to IUPAC classification, the obtained isotherms belong to a type IV isotherm and indicate textural heterogeneity (Xiong et al., 2010). The textural characteristics of the investigated sorbents are presented in Table 1. The addition of the surfactant P123 leads to a significant increase of specific surface area and total pore volume of the HAP P123 in comparison with untreated HAP.

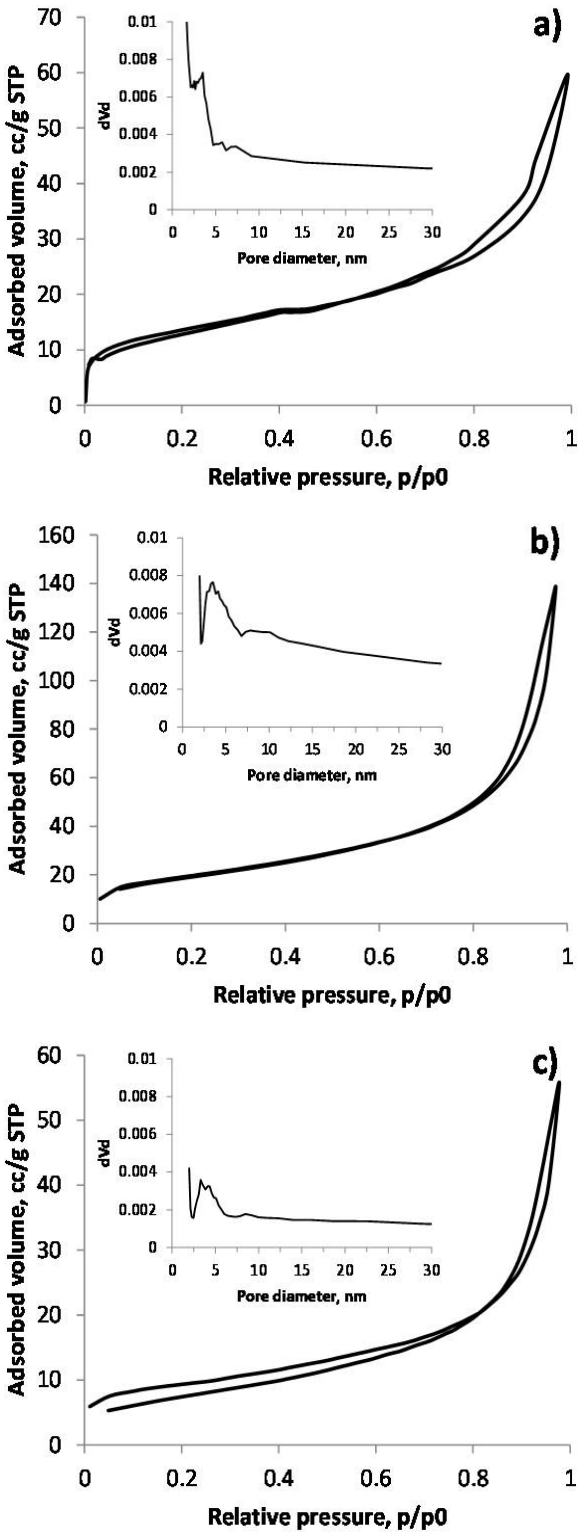

Fig. 1. Nitrogen sorption isotherm and corresponding pore size distributions for the synthesized HAP samples: (a) represent HAP, (b) HAP P123 and (c) HAP F127

At the addition of F127, the pore volume remains almost on the level of untreated HAP, while the specific surface area of sorbent was reduced. A decrease in surface area and pore volume could be

related to the fact that high concentration of the F127 surfactant (of 2.5%) may provoke an intensive extrusion instead of the formation of micelles (at CMC of 0.725%) (Mohammad et al., 2015), thus resulting in a reduction of surface area and total pore volume.

SEM microphotographs of the analyzed sorbents are presented in Fig. 2. Fig. 3 represents the FTIR spectra of HAP and its two modifications. The peaks observed at 1020, 1030 and 1000 cm^{-1} for HAP, HAP P123, and HAP F127 are due to the asymmetric stretching vibration of P–O bond of phosphate PO_4^{3-} group (Sairam Sundaram et al., 2009). The bands detected at 557, 559 and 561 cm^{-1} are attributed to the bending vibration of O–P–O bond of the phosphate PO_4^{3-} group (Sheha et al., 2016). The small bands at 3634 cm^{-1} are assigned to the O–H stretching vibration of surface P–OH groups, while bands at 599 cm^{-1} are ascribed to the stretching and liberational mode of OH group vibration (Sheha et al., 2016). In FTIR spectra of HAP P123 and HAP F127 were observed a slight increase of the intensity of deformation bands of PO_4^{3-} ions. Depending upon solution pH, such surface sites can act as a weak acid or base and gain or lose a proton (Sheha et al., 2016).

Table 1. Textural properties of the synthesized sorbents

Sorbent	***Specific surface, m^2/g***	***Pore Volume, cm^3/g***	***Pore diameter, nm***
HAP	47.251±0.1	$6.48 \cdot 10^{-2}$±0.01	3.12 (2.5-5.0)
HAP P123	69.153±0.1	$1.59 \cdot 10^{-1}$±0.01	3.50 (2.5-6.0)
HAP F127	31.719±0.1	$6.18 \cdot 10^{-2}$±0.01	4.13 (2.5-5.0)

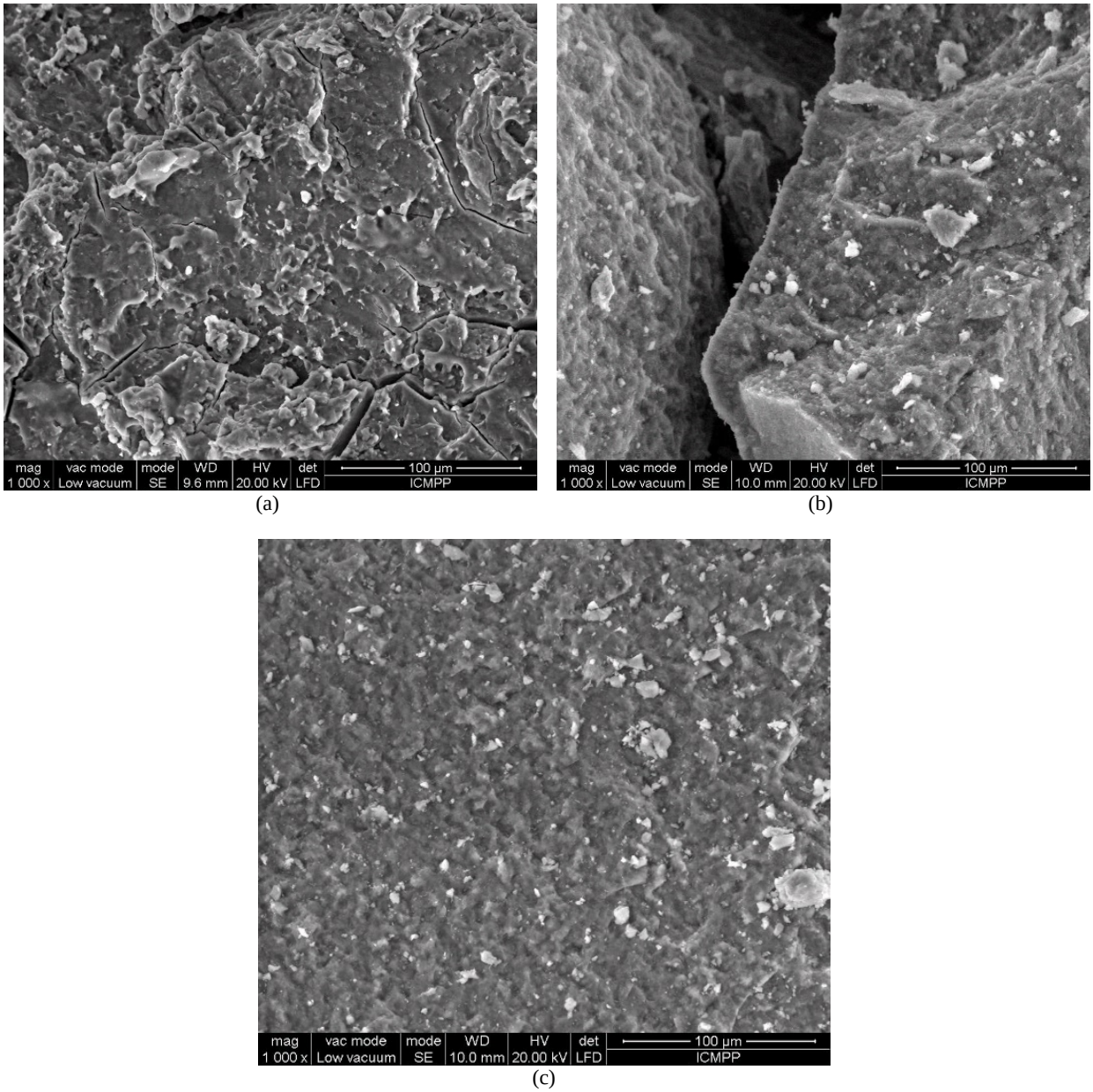

Fig. 2. SEM microphotographs of the HAP samples: (a) represent HAP, (b) HAP P123 and (c) HAP F127

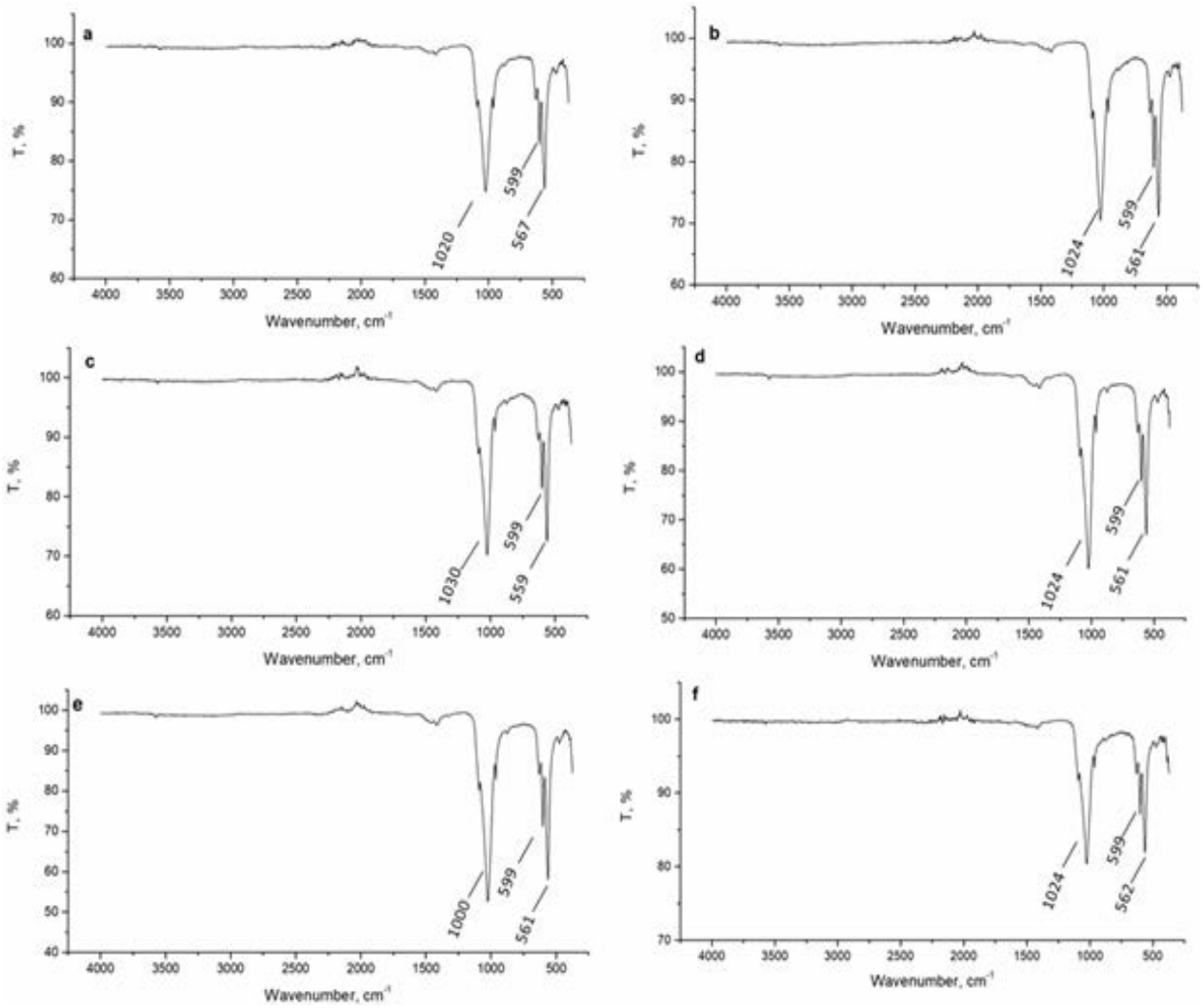

Fig. 3. FTIR spectra of sorbents: (a) represent HAP control, (b) HAP loaded with V, (c) HAP P123 control, (d) HAP P123 loaded with V, (e) HAP F127 control, (f) HAP F127 loaded with V

3.2. Effect of pH dependence of sorption process

The effectiveness of vanadium ions sorption depends on its speciation in an aqueous solution and the surface charge of the adsorbent. At pH below 3.0 vanadium exists in solution in VO_2^+ form, between pH 4.0 and 11.0 the anionic forms predominate (neutral $VO(OH)_3$ and anionic species $V_{10}O_{26}(OH)^{3-}$, $V_{10}O_{27}(OH)^{5-}$, $V_{10}O_{28}^{6-}$ and other mono or poly vanadate species $VO_2(OH)_2^-$, $VO_3(OH)^{2-}$, VO_4^{3-}, $V_2O_6(OH)^{3-}$, $V_2O_7^{4-}$, $V_3O_9^{3-}$ and $V_4O_{12}^{4-}$) (Peng et al., 2020). The effect of initial pH on vanadium(V) removal by the HAP and its two modifications HAP P123 and HAP F127 is shown in Fig. 4.

The maximum vanadium(V) removal was achieved at pH 2.0 for all analyzed sorbents. This is an agreement with (Peng et al., 2020; Vega et al., 1999; 2003) studies. HAP adsorption capacity for vanadium ions was comparable with the values obtained by (Vega et al., 1999; 2003), while whose of HAP P123 and HAP F127 was almost two times higher. The efficiency of vanadium (V) removal changed in the following order HAP P123 (70.4%)> HAP F127 (47.2%)> HAP (44.3%).

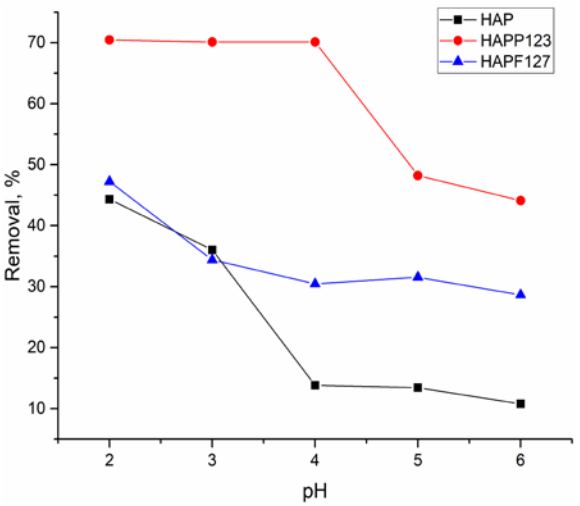

Fig. 4. Removal of vanadium ions at different initial pH (at T= 20 ^{0}C; sorbent dosage 0.02 g; adsorption time 1 h)

Higher sorption of vanadium (V) by HAP P123 can be explained by its higher specific surface area and volume of pores. Since adsorption is a surface reaction, a high surface area is often seen as an

important characteristic of the adsorbent. Porous materials, which have a high surface area are characterized by a high adsorption capacity (Suresh Kumar et al., 2019). Vega et al. (1999) showed that VO^{2+} ions are specifically adsorbed to OH groups. This evidence was supported by the authors' further research, in which they showed that in IR spectra of HAP at different concentrations of adsorbed V a systematic decrease of the OH stretching band intensities while adsorbed VO^{2+} increased. The bands of PO_4 and CO_3 groups were not modified. The authors also proposed another mechanism of vanadium specific adsorption onto the positively charged functional groups on the sorbent surface with the formation of an inner sphere surface complex (Vega et al., 2003). Dikanov et al. (2013) suggested that vanadium sorption can occur by o a diffusion of vanadyl ions inside the hydroxyapatite and its preferable equatorial coordination with phosphate oxygen atoms.

For HAP P123 the high rate of vanadium(V) removal was also found at pH 3 and 4. By increasing pH up to 3.0-4.0, the anion species of vanadium can be adsorbed by electrostatic attraction (Sharififard and Soleimani, 2015). With the increase of pH up to 6.0 vanadium(V) removal efficiency significantly decreased for all sorbents, due to precipitation of oxovanadium hydroxide, $VO(OH)_2$ (Vega et al., 2003) as well as increase of OH concentration and competition with vanadium anions for the available surface sites (Zhang et al., 2019).

3.3. Effect of contact time on the sorption process

The study of the effect of contact time on vanadium(V) ions removal showed that sorption has increased considerably in the first 60 min of interaction and then the equilibrium was achieved (Fig. 5). At equilibrium, 70% of vanadium ions were removed from the solution by HAP P123, 47% by HAP F127 and 43% by HAP. The high removal efficiency of HAP P123 is associated with its high surface area.

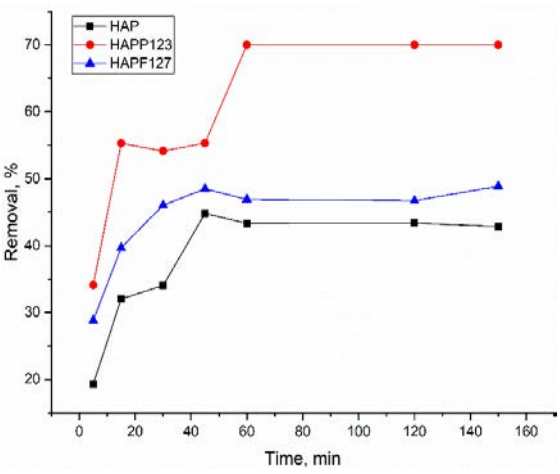

Fig. 5. Adsorption of vanadium ions as the function of time (at T= 20 ^{0}C, sorbent dosage 0.02 g, pH= 2.0)

Four kinetic models: pseudo-first-order, pseudo-second-order, Elovich, and intra-particle diffusion models were applied to describe vanadium sorption. The models are expressed by the Eqs. (3-6):

Pseudo- first-order model (Eq. 3) (Ho, 2004):

$$q = q_e(1 - e^{-k_1 t}) \quad (3)$$

where q_e and q_t are the amounts of vanadium(V) (mg/g) adsorbed at equilibrium and at t (min) time, respectively, and k_1 (1/min) is the rate constant of pseudo-first-order.

Pseudo-second order model (Eq. 4) (Ho and McKay, 1999):

$$q = \frac{q_e^2 k_2 t}{1 + q_2 k_2 t} \quad (4)$$

where k_2 (g/mg·min) is the rate constant of second order.

Elovich model (Eq. 5) (Boulaiche et al., 2019):

$$q_t = \frac{1}{\beta}\ln(\alpha\beta) + \frac{1}{\beta}\ln(t) \quad (5)$$

where α and β are the Elovich equation constants.

Weber and Morris intraparticle diffusion model (Eq. 6):

$$q = k_{diff} \cdot t^{0.5} + C_i \quad (6)$$

where k_{diff} is the rate parameter of i step (mg/g·min$^{1/2}$), C_i is the intercept of i step, giving an idea about the thickness of the boundary layer.

The experimental kinetic parameters calculated according to the indicated models (Fig. 6) and the coefficients of determination values are listed in Table 2. According to coefficients of determination values, the adsorption of vanadium(V) ions onto HAP and HAP F127 follows the pseudo-second-order kinetic model, while for HAP P123 pseudo-first-order model.

Table 2. Kinetic parameters of the adsorption of vanadium (V) ions

Kinetic model	***Sorbent***		
	HAP	***HAP F127***	***HAP P123***
Pseudo first order			
$q_{e,\,exp}$ (mg·g^{-1})	2.00	1.9	2.6
$q_{e,\,calc}$ (mg·g^{-1})	1.93	1.92	2.47
k_1 (min^{-1})	0.095	0.17	0.18
R^2	0.87	0.91	0.92
Pseudo second order			
$q_{e,\,exp}$ (mg·g^{-1})	2.0	1.9	2.6
$q_{e,\,calc}$ (mg·g^{-1})	2.1	2.03	2.64
k_2 (g· mg^{-1}·min^{-1})	0.067	0.14	0.11
R^2	0.91	0.98	0.90
Elovich model			
α $q_{e,\,calc}$ (mg·g^{-1})	1.53	17.8	23.1
β (g· mg^{-1}·min^{-1})	3.07	4.5	3.48
R^2	0.8	0.81	0.71
Intraparticle difussion			
K_{diff} (mg/g·min$^{1/2}$)	0.09	0.06	0.08
C_1	1.02	1.33	1.73
R^2	0.57	0.55	0.48

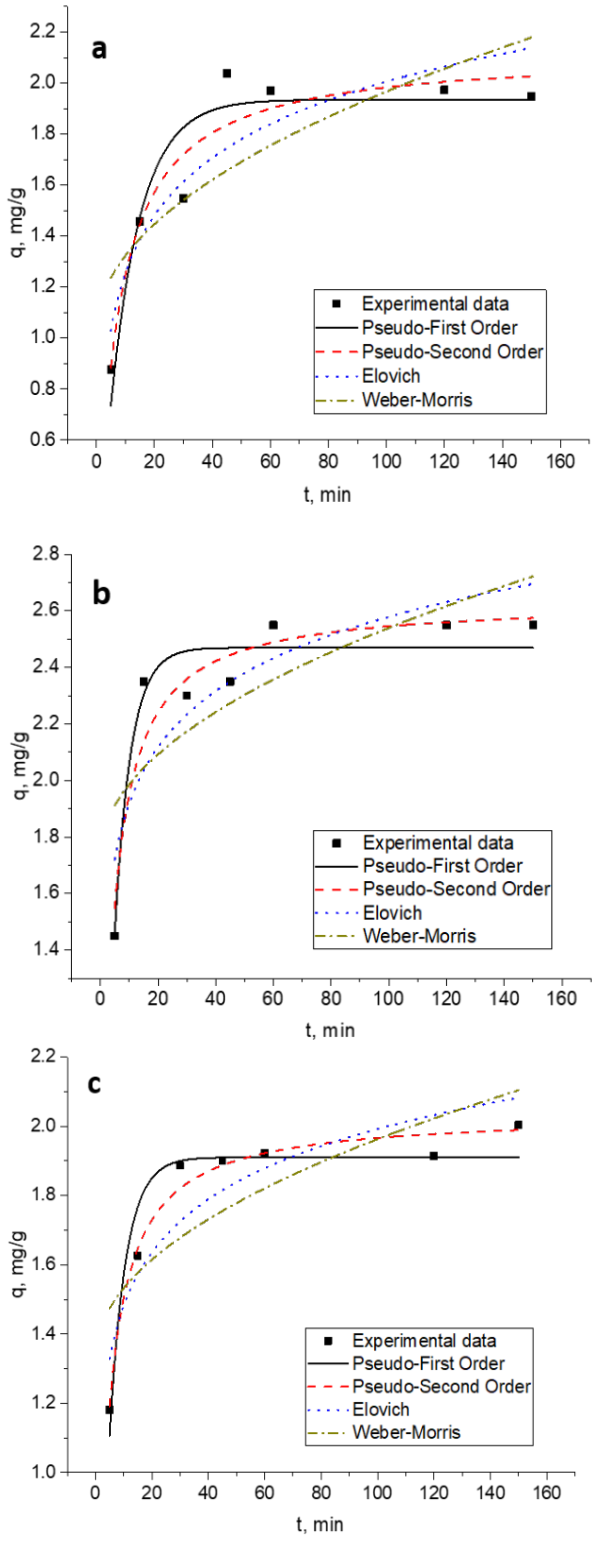

Fig. 6. Kinetics of vanadium sorption on (a) HAP, (b) HAP P123 and (c) HAP F127

The pseudo-second-order model is based on the assumption that the rate-limiting step of the adsorption may be chemical adsorption or chemisorption involving valency forces through sharing or exchange of electrons between sorbent and sorbate (Ho and McKay, 1999). The pseudo-first-order kinetic model assumes that the rate of occupation of sorption sites is proportional to the number of unoccupied sites (Zinicovscaia et al., 2020). It should be mentioned that adsorption capacity q_e calculated from both models is in good agreement with the experimental data. Coefficients of determination calculated for Elovich and Weber and Morris intra-particle diffusion models were much lower. The validity of the pseudo-second-order model for vanadium ion adsorption kinetics on CAC and Fe–AC was shown in Sharififard and Soleimani (2015) study. The sorption of vanadium ions by ferric groundwater treatment residual was better described by the Elovich model, which is generally useful to describe chemisorption on highly heterogeneous adsorbents (Zhang et al., 2019). Vanadium removal by anion exchange resins follows the pseudo-first-order model (Gomes et al., 2017).

3.4. Effect of the initial concentration of vanadium ions on the sorption process

The data on the effect of initial vanadium(V) concentration on the adsorption capacity of studied sorbents (Fig. 7) show that increase of vanadium concentration in solution from 10 to 100 mg/L leads to an increase in metal ions sorption. Thus, the total concentration of vanadium taken up by HAP P123 was 24.1 mg/g compared to 18.10 mg/g and 14.20 mg/g for HAP and HAP F127, respectively. The higher sorption capacity HAP P123 in comparison with HAP and HAP F127 can be explained by its higher specific surface area.

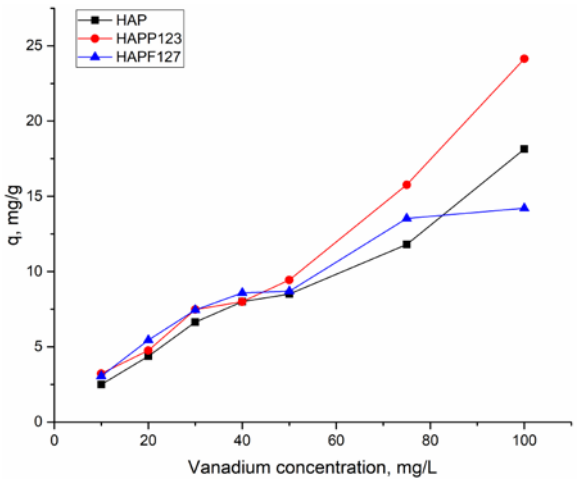

Fig. 7. Adsorption of vanadium ions as the function of vanadium concentration in solution (at T =20 ^{0}C; sorbent dosage 0.02 g, time of contact 1 h, pH =2.0)

The models: Langmuir, Freundlich, and Temkin adsorption isotherm were applied to describe the mechanism of vanadium ion adsorption by studied adsorbents. The Langmuir model suggests monolayer adsorption, with no lateral interaction between the sorbed molecules (Namasivayam and Sangeetha, 2006) and is expressed by the Eq. (7):

$$q_e = \frac{q_m b C_e}{1 + b C_e} \qquad (7)$$

where: C_e is metal ions concentration at equilibrium (mg/L); q_e is amount of metal adsorbed at equilibrium (mg/g); q_m is maximum adsorption capacity of the sorbent (mg/g) and b is Langmuir adsorption constant (L/mg). K_L is a constant that is important in calculating the dimensional parameter (R_L) that explains the favorability of the adsorption process. R_L is calculated using Eq. (8):

$$R_L \frac{1}{1+K_L C_O} \quad (8)$$

$R_L > 1$ the adsorption process is unfavorable; $R_L = 1$ adsorption is linear; $0 < R_L < 1$ adsorption process is favorable; $R_L = 0$ adsorption is irreversible.

The non-linearized form of Freundlich isotherm model is given in the Eq. (9):

$$q_e = K_F C^{\frac{1}{n}} \quad (9)$$

where q_e is amount of metal adsorbed at equilibrium (mg/g); C_e is concentration of metal ions in aqueous solution at equilibrium (mg/L); K_F and n are Freundlich constants that include factors that affect adsorption capacity and adsorption intensity, respectively.

The Temkin isotherm is usually applied for heterogeneous surface energy systems. Assumptions of the model are: 1-adsorption is exponential, and 2-adsorption is a single layer (Dehghani et al., 2018). The model is described by Eq. (10):

$$q_e = \frac{RT}{b_T} \ln(a_T C_e) \quad (10)$$

where: $1/b_T$ indicates the sorption potential of the sorbent, and K_T is Temkin constant. In the above equation, $B=RT/b_T$ is a constant showing heat of sorption (J/mol).

The coefficients of determination (R^2) and isotherm parameters are given in Table 3 and isotherms plots in Fig. 8. The higher values of coefficients of determination were obtained for the Freundlich model (R^2 of 0.98), indicating that the model provided the best-fitting for the equilibrium data of vanadium ion adsorption by HAP, HAP P123, and HAP F127. Applicability of the Freundlich model may be attributed to the coexistence of different sorption sites and/or different sorption mechanisms or the sorption of vanadium ions that have led to heterogeneous adsorption (Sharififard and Soleimani, 2015). The Freundlich constant n values higher than 1.0 suggest that vanadium adsorption was privilege favorable (Peng et al., 2020).

The maximal theoretical adsorption capacity of the analyzed sorbent calculated from the Langmuir model increased in the following order HAP P123> HAP F127>HAP. The R_L values between 0 and 1 indicate favorable adsorption. The calculated maximum uptake capacity was higher than experimentally obtained values, indicating that vanadium adsorption by HAP and its two modifications would proceed at higher vanadium concentrations (Zinicovscaia et al., 2018). Coefficients calculated for the Temkin model were lower than those obtained for Langmuir and Freundlich models for sorbents HAP and HAP P123, while for HAP F127 it was on the level of the abovementioned models. The positive value of b_T indicates the endothermic character of vanadium sorption (Ahmad et al., 2014).

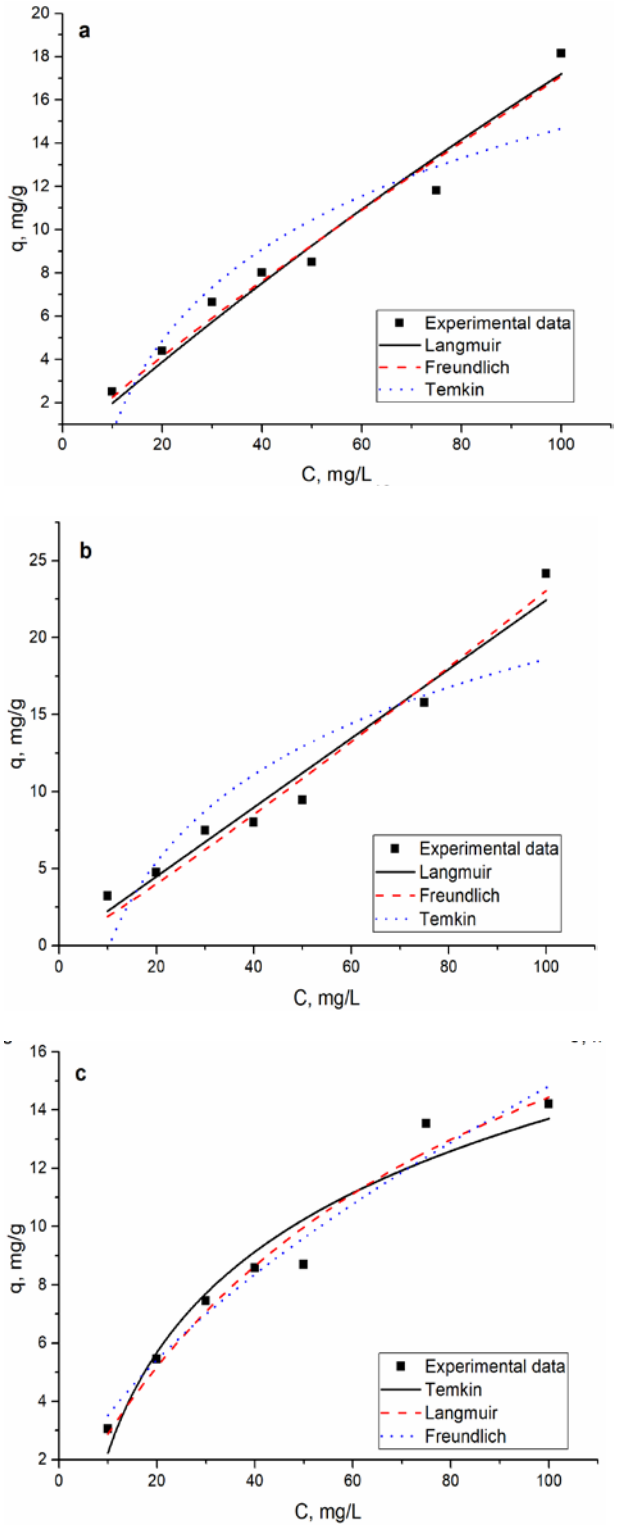

Fig. 8. Isotherms of vanadium sorption on: (a) HAP, (b) HAP P123 and (c) HAP F127

Table 3. Adsorption isotherm parameters

Model	*HAP*	*HAP F127*	*HAP P123*
Langmuir			
q_m (mg·g^{-1})	20.0	26.0	32.8
b (L·g^{-1})	0.002	0.012	0.0006
R_L	0.92	0.86	0.88
R^2	0.96	0.96	0.96
Freundlich			
K_F	0.29	0.84	0.15
n	1.33	1.6	0.92
R^2	0.98	0.98	0.98
Temkin			
K_T	0.11	0.49	0.11
b_T	0.39	0.16	0.29
B	6.2	15.2	8.1
R^2	0.83	0.93	0.74

Vanadium sorption by synthesized and commercial calcium hydroxyapatite fit well Langmuir model (Ordinartsev et al., 2016; Vega et al., 1999; 2003). The process of vanadium sorption was described by authors as physical sorption. A comparison of the sorption capacity of analyzed sorbents and data obtained for other sorbents are presented in Table 4. This comparison indicates that studied adsorbents exhibit a reasonable capacity for vanadium adsorption from aqueous solutions.

3.5. Influence of temperature on the adsorption process

The effect of the temperature on the adsorption processes of vanadium ions on the analyzed sorbents was investigated at a temperature range of 20 – 50°C. From the data presented in Fig. 9, it can be observed that the increase of temperature has a slight effect on vanadium(V) removal by HAP and HAP P123 sorbents. The observed trend could be due to the nature of the sorbent particles (Sharififard and Soleimani, 2015). In the case of HAP F127 rise of temperature from 20 to 30ºC resulted in the increase of vanadium ions removal by 13%, and further temperature increase did not affect it significantly.

To understand the nature of the adsorption process the Gibbs free energy change (ΔG°), enthalpy (ΔH°) and entropy (ΔS°) values were calculated according to Eqs. (11-12):

$$\ln K_d = \frac{\Delta S^0}{R} - \frac{\Delta H^0}{RT} \quad (11)$$

$$\Delta G^0 = \Delta H^0 - T\Delta S^0 \quad (12)$$

where K_d is the distribution coefficient and it is calculated to Eq. (13):

$$K_d = \frac{(C_0 \ C_e)V}{mC_e} \quad (13)$$

where C_0 is initial concentration of vanadium, (mg/L), C_e is vanadium concentration in aqueous solution at equilibrium, (mg/L), V is the volume of aqueous solution (L), and m is sorbent mass (g).

The values of ΔH^o and ΔS^o were calculated from the slope and the ordered intercept of the $1/T$ function representation of lnK_d (Fig. 10). The results obtained are presented in Table 5.

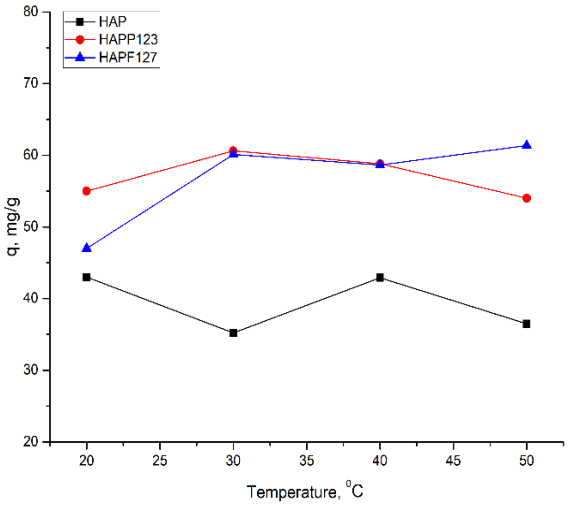

Fig. 9. Adsorption of vanadium ions as the function of temperature (sorbent dosage 0.02 g, interaction time 1 h, pH =2.0)

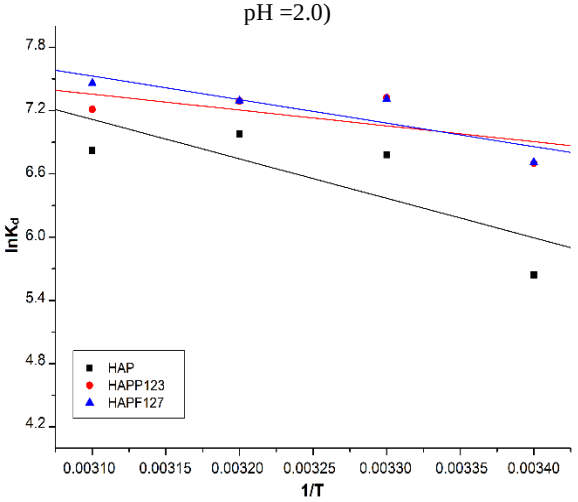

Fig. 10. Dependence of distribution coefficient on the temperature

For all three sorbents, the obtained ΔH^o and of ΔS^o values were positive, which indicated the endothermic nature of vanadium(V) adsorption (Tounsadi et al., 2015). The positive values show a high affinity of the three sorbents toward vanadium(V) ions. It is known that physical adsorption is generally an exothermic reaction. Hence, the logical cause of the observation is that the adsorption should include some endothermic chemical reactions, which are supported by increasing adsorptive capacity with rising temperature (Wang L. et al., 2020).

The negative values of ΔG° demonstrated that adsorption is a spontaneous process. For all sorbents with the increase of the temperature, the decrease of ΔG° takes place, indicating a higher adsorption impetus in higher temperature (Li et al., 2009).

Table 4. Comparison of sorption capacity of different sorbents toward vanadium ions

Sorbent	*pH*	q_m, *mg/g*	*Reference*
HAP	2	20	Present study
HAP P123	2	32.6	Present study
HAP F127	2	26	Present study
Granulated Activated Carbon	2	370	Ahmad et al. (2014)
Calcium hydroxyapatite	3.5	13.4 μmol/g	Vega et al. (1999)
Commercial calcium hydroxyapatite	3.5	19 μmol/g	Vega et al. (2003)
Activated charcoal	-	16	Ordinartsev et al. (2016)
Granulated Activated Carbon	11.5	4.99	Chaudhari (2009)
Fe-GWTR	4	15.6	Zhang et al. (2019)
Anion exchange resins	2	27	Gomes et al. (2017)
Activated carbon	4	37.17	Doğan and Aydin (2014)
Humic acid	4.7	19.2	Yu et al. (2018)
A cellulose-based anion exchanger	4-6	197.75	Anirudhan et al. (2009)
Melamine	1.0	1428	Peng et al. (2017)
Commercial activated carbon	4.7	37.87	Sharififard and Soleimani (2015)
Ferric oxide-hydroxide–activated carbon nanocomposite	4	119.01	Sharififard and Soleimani (2015)

Table 5. Thermodynamic parameters of the adsorption process of vanadium (V) ions

Sorbent	*ΔH°, kJ/mol*	*ΔS°, kJ/mol·K*	*ΔG°, kJ/mol*			
			293	*303*	*313*	*323*
HAP	31.1	0.155	-14.5	-16.0	-17.6	-19.1
HAP 127	18.5	0.120	-16.5	-17.7	-18.9	-20.1
HAP 123	12.5	0.099	-16.8	-17.8	-18.8	-19.8

4. Conclusions

Vanadium(V) ions removal from aqueous solutions by untreated hydroxyapatite and its two modifications was studied. Vanadium sorption was affected by contact time, solution pH, temperature, and initial concentration of metal ions.

Adsorption kinetics was better described by the pseudo-second-order model for HAP and HAP F127 and by the pseudo-first-order kinetic model for HAP P123. Adsorption of vanadium (V) was fitted well by the Freundlich isotherm models for all sorbents and for HAP F127 by the Temkin isotherm model as well.

The adsorption process is endothermic ($\Delta H° >$ 20 kJ/mol) and spontaneous (the increase of the negative values of $\Delta G°$ with the increase of temperature). Obtained data shows that HAP modification with the surfactants P123 resulted in a slight increase of its sorption capacity toward vanadium ions. Studied sorbents can be considered as possible candidates for efficient vanadium ions removal from wastewater.

Acknowledgments
This work was supported by JINR project, no. 03-4-1128-2017/2019, item 100.

References

Ahmad M.A., Puad N.A.A., Bello O.S., (2014), Kinetic, equilibrium and thermodynamic studies of synthetic dye removal using pomegranate peel activated carbon prepared by microwave-induced KOH activation, *Water Resources and Industry*, **6**, 18-35.

Anirudhan T.S., Jalajamony S., Divya L., (2009), Efficiency of amine-modified poly (glycidyl methacrylate)-grafted cellulose in the removal and recovery of vanadium (V) from aqueous solutions, *Industrial & Engineering Chemistry Research*, **48**, 2118-2124.

Arsad M.S., Lee P.M., Hung L.K., (2011), *Synthesis and Characterization of Hydroxyapatite Nanoparticles and β-TCP Particles*, 2nd International Conference on Biotechnology and Food Science, IPCBEE, **7**, 184-188.

Bazargan-Lari R., Zafarani H.R., Bahrololoom M.E., Nemati A., (2014), Removal of Cu (II) ions from aqueous solutions by low-cost natural hydroxyapatite/chitosan composite: Equilibrium, kinetic and thermodynamic studies, *Journal of the Taiwan Institute of Chemical Engineers*, **45**, 1642-1648.

Boulaiche W., Hamdi B., Trari M., (2019), Removal of heavy metals by chitin: equilibrium, kinetic and thermodynamic studies, *Applied Water Science*, **9**, 39, https://doi.org/10.1007/s13201-019-0926-8.

Chaudhari U.E., (2009), Removal of Vanadium (V) from water by adsorption using GAC loaded with ethylene di-amine tetra acetic acid (EDTA) and nitrilo tri-acetic acid (NTA), *Oriental Journal of Chemistry*, **25**, 799-803.

Dehghani M.H., Tajik S., Panahi A., Khezri M., Zarei A., Heidarinejad Z., Yousefi M., (2018), Adsorptive removal of noxious cadmium from aqueous solutions using poly urea-formaldehyde: a novel polymer adsorbent, *MethodsX*, **5**, 1148-1155.

Dikanov S.A., Liboiron B.D., Orvig C., (2013), VO^{2+}-hydroxyapatite complexes as models for vanadyl coordination to phosphate in bone, *Molecular Physics*, **111**, 2967-2979.

Doğan V., Aydın S., (2014), Vanadium (V) removal by adsorption onto activated carbon derived from starch industry waste sludge, *Separation Science and Technology*, **49**, 1407-1415.

Fernando M.S., Nali De Silva R.M., Nali De Silva K.M., (2015), Synthesis, characterization, and application of nano hydroxyapatite and nanocomposite of hydroxyapatite with granular activated carbon for the

removal of Pb^{2+} from aqueous solutions, *Applied Surface Science*, **351**, 95-103.

Gomes H.I., Jones A., Rogerson M., Greenway G.M., Lisbona D.F., Burke I.T., Mayes W.M., (2017), Removal and recovery of vanadium from alkaline steel slag leachates with anion exchange resins, *Journal of Environmental Management*, **187**, 384-392.

He Q., Si S., Zhao J., Yan H., Sun B., Cai Q., Yu Y., (2018), Removal of vanadium from vanadium-containing wastewater by amino modified municipal sludge derived ceramic, *Saudi Journal of Biological Sciences*, **25**, 1664-1669.

Ho Y.S., (2004), Citation review of Lagergren kinetic rate equation on adsorption reactions, *Scientometrics*, **59**, 171-177.

Ho YS., McKay G., (1999), Pseudo-second order model for sorption processes, *Process Biochemistry*, **34**, 451-65.

Liu D.M., Troczynski T., Tseng W.J., (2001), Water-based sol-gel synthesis of hydroxyapatite: process development, *Biomaterials*, **22**, 1721-1730.

Mohammad N.F., Othman R., Yeoh F.Y., (2015), Controlling the pore characteristics of mesoporous apatite materials: Hydroxyapatite and carbonate apatite, *Ceramics International*, **41**, 10624-10633.

Namasivayam C., Sangeetha D., (2006), Removal and recovery of vanadium (V) by adsorption onto $ZnCl_2$ activated carbon: kinetics and isotherms, *Adsorption*, **12**, 103-117.

Ordinartsev D.P., Sviridov A.V., Sviridov V.V., (2016), Thermodynamic description of the process of vanadium adsorption in carbon sorbent, *Bulletin of the South Ural State University Series 'Metallurgy'*, **16**, 14-22.

Paz A., Guadarrama D., López M., E González J., Brizuela N., Aragón J., (2012), A comparative study of hydroxyapatite nanoparticles synthesized by different routes, *Química Nova*, **35**, 1724-1727.

Peng H, Shang Q., Chen R., Zhang L., Chen Y., Guo J., (2020), Step-adsorption of Vanadium (V) and Chromium (VI) in the leaching solution with melamine, *Scientific Reports*, **10**, 6326, https://doi.org/10.1038/s41598-020-63359-z.

Peng H., Liu Z., Tao C., (2017), Adsorption kinetics and isotherm of vanadium with melamine, *Water Science and Technology*, **75**, 2316-2321.

Piccirillo C., Pereira S.I.A., Marques A.P., Pullar R.C., Tobaldi D.M., Pintado M.E., Castro P.M., (2013), Bacteria immobilization on hydroxyapatite surface for heavy metals removal, *Journal of Environmental Management*, **121**, 87-95.

Ramanan S.R., Venkatesh R., (2004), A study of hydroxyapatite fibers prepared via sol-gel route, *Materials Letters*, **58**, 3320-3323.

Sairam Sundaram C., Viswanathan N., Meenakshi S., (2009), Fluoride sorption by nano-hydroxyapatite/chitin composite, *Journal of Hazardous Materials*, **172**, 147-151.

Saoiabi S., Gouza A., Bouyarmane H., Laghzizil A., Saoiabi A., (2016), Organophosphonate-modified hydroxyapatites for Zn(II) and Pb(II) adsorption in relation of their structure and surface properties, *Journal of Environmental Chemical Engineering*, **4**, 428-33.

Sharififard H., Soleimani M., (2015), Performance comparison of activated carbon and ferric oxide-hydroxide-activated carbon nanocomposite as vanadium (V) ion adsorbents, *RSC Advances*, **5**, 80650-80660.

Sheha R.R., Moussa S.I., Attia M.A., Sadeek S.A., Someda, H.H., (2016), Novel substituted hydroxyapatite nanoparticles as a solid phase for removal of Co(II) and Eu(III) ions from aqueous solutions, *Journal of Environmental Chemical Engineering*, **4**, 4808-4816.

Suresh Kumar P., Korving L., Keesman K.J., van Loosdrecht M.C.M., Jan Witkamp G., (2019), Effect of pore size distribution and particle size of porous metal oxides on phosphate adsorption capacity and kinetics, *Chemical Engineering Journal*, **358**, 160-69.

Tounsadi H., Khalidi A., Abdennouri M., Barka N., (2015), Biosorption potential of *Diplotaxis harra* and *Glebionis coronaria* L. biomasses for the removal of Cd(II) and Co(II) from aqueous solutions, *Journal of Environmental Chemical Engineering*, **3**, 822-830.

Vega E.D., Pedregosa J.C., Narda G.E., (1999), Interaction of oxovanadium (IV) with crystalline calcium hydroxyapatite: surface mechanism with no structural modification, *Journal of Physics and Chemistry of Solids*, **60**, 759-766.

Vega E.D., Pedregosa J.C., Narda G.E., Morando, P.J., (2003), Removal of oxovanadium (IV) from aqueous solutions by using commercial crystalline calcium hydroxyapatite, *Water Research*, **37**, 1776-1782.

Wang L., Shi C., Wang L., Pan L., Zhang X., Zou J.J., (2020), Rational design, synthesis, adsorption principles and applications of metal oxide adsorbents: a review, *Nanoscale*, **27**, 4790-4815.

Wang M., Zhang K., Wu M., Wu Q., Liu J., Yang J., Zhang J., (2019), Unexpectedly high adsorption capacity of esterified hydroxyapatite for heavy metal removal, *Langmuir*, **35**, 16111-16119.

Wang P., Li C., Gong H., Jiang X., Wang H., Li K., (2010), Effects of synthesis conditions on the morphology of hydroxyapatite nanoparticles produced by wet chemical process, *Powder Technology*, **203**, 315-321.

Xiong L., Yan X.M., Mei P., (2010) Synthesis and characterization of a ZrO_2/AC composite as a novel adsorbent for dibenzothiophene, *Adsorption Science & Technology*, **28**, 341-350.

Yu Y., Liu M., Yang J., (2018), Characteristics of vanadium adsorption on and desorption from humic acid, *Chemistry and Ecology*, **34**, 548-564.

Zhang R., Leiviskä T., Tanskanen J., Gao B., Yue Q., (2019), Utilization of ferric groundwater treatment residuals for inorganic-organic hybrid biosorbent preparation and its use for vanadium removal, *Chemical Engineering Journal*, **361**, 680-689.

Zinicovscaia I., Yushin N., Abdusamadzoda D., Grozdov D., Shvetsova M., (2020), Efficient removal of metals from synthetic and real galvanic zinc–containing effluents by brewer's yeast *Saccharomyces cerevisiae*, *Materials*, **13**, 3624, https://doi.org/10.3390/ma13163624.

Zinicovscaia I., Yushin N., Shvetsova M., Frontasyeva M., (2018), Zinc removal from model solution and wastewater by *Arthrospira (spirulina) platensis* biomass, *International Journal of Phytoremediation*, **20**, 901-908.

Zwolak I., (2020), Protective effects of dietary antioxidants against vanadium-induced toxicity: a review, *Oxidative Medicine and Cellular Longevity*, **4**, 1-14.